COBEM 2021 26th International Congress of Mechanical Engineering
November 22-26, 2021, Virtual Congress, Brazil

COB-2021-1415
EXPERIMENTAL ANALYSIS OF DOWNWARD VERTICAL AIR-WATER ANNULAR FLOW

Ana Luiza B. Santana
Eduardo N. dos Santos
Rafael F. Alves
Dalton Bertoldi
Marco J. da Silva
Moisés A. Marcelino Neto
Rigoberto E. M. Morales

Multiphase Flow Research Center (NUEM), Federal University of Technology – Paraná (UTFPR), Rua Deputado Alencar Furtado 5000, Bloco N, CEP 81280340, Curitiba, Brazil
anabeltraos@gmail.com, e.n.santos@ieee.org, rafael.alves@funtefpr.org.br, daltonbertoldi@utfpr.edu.br, mdasilva@utfpr.edu.br, mneto@utfpr.edu.br, rmorales@utfpr.edu.br

Abstract. *Annular flow is characterized by a continuous, fast-moving gas core with a liquid film wetting the pipe wall. This flow pattern has a wavy interface whose waves were formed by the high interfacial shear stress between the phases. The literature shows an extensive number of studies for upward vertical annular flows and a lack of interest in downward annular flows. Regarding those latter, the majority of the works use limited experimental apparatuses with regard to the length–to-diameter ratio (L/D). Therefore, because of this restriction, a flow conditioner that induces the annular flow patterns is frequently adopted. It is known that depending on the type of flow conditioner the characteristics of the interfacial structures of the two-phase flow pattern and the trend of the flow to evolve in the downstream axial direction can be influenced. In this regard, experiments to analyze the main characteristics of downward vertical air-water annular flow in a 26-mm ID, 14-m length pipe were carried out. Tests using two different types of flow conditioners to evaluate the influences of the phase injection on the features of the liquid film and downstream evolution of the flow at two test sections (placed at 90D and 335D from the flow conditioner outlet) were performed. A non-intrusive conductance sensor and a high-speed camera were deployed in the test sections to measure the characteristics of the liquid film. Twenty-one combinations of air and water superficial velocities ranging from 10 m/s to 20 m/s and 0.05 m/s to 0.25 m/s, respectively, were investigated. Analysis of the liquid film time series provided liquid film features such as the average film thickness, liquid film roughness, disturbance wave velocity, and disturbance wave frequency. Results showed variations for all annular flow features evaluated in the axial direction. Besides, the flow conditioner that not induces the annular flow, affects the flow at the test section closer to phase entrance (90D).*

Keywords: *downward vertical, annular flow, liquid film, flow conditioner.*

1. INTRODUCTION

The annular flow pattern is oftentimes observed in pieces of industrial equipment such as nuclear reactor systems, evaporators, condensers, and in the oil and gas industry (Hewitt, G F and Hall-Taylor, 1970). According to Barnea, Shoham and Taitel (1982), annular is the most common flow regime in vertical downward flows. In particular, when only liquid flows in a downward vertical pipe with a low flow rate, a thin liquid film forms on the pipe wall, characterizing the so-called falling film flow pattern. A literature review on downward two-phase flow summarizing data, models, and flow mechanics was presented by Lokanathan and Hibiki (2016). Qiao, Mena and Kim (2017) investigated the geometric effects of three types of inlets on global and local characteristics of downward vertical air-water two-phase flows in a test facility with a 50.8-mm ID, 3.35-m long (66D) pipe observing that the inlet influences the flow parameters analyzed.

The liquid film presents waves on the gas-liquid interface, which were classified by Chu and Dukler (1975) into two classes of random waves: the large, also referred to as disturbance waves; and the small ones or ripples waves, which cover the remaining portion of the liquid film that is identified as the substrate or base film. In addition, the disturbance waves travel along with the liquid film at velocities greater than those of the substrate film velocity. Fershtman et al. (2021) experimentally examined the interfacial structure of inclined upward annular flows using a multilayered conductance liquid sensor and proposed a new criterion to differentiate disturbance waves from ripples based on a statistical analysis of probability density function distributions. The authors used a 10-m long, 24-mm ID experimental

facility with the test section placed 310D apart from the pipe inlet, but provided no information about the type of flow conditioner.

For vertical downward annular flows (VDAF), Webb and Hewitt (1975) proposed a flow regime map based on the topological characteristics of the gas-liquid interface. The authors experimentally observed four different flow regimes named ripple, regular disturbance wave, dual wave, and thick ripple. In a recent work, Zadrazil, Matar and Markides (2014), using Planar Laser-Induced Fluorescence (PLIF), identified a new VDAF regime named *disturbance wave regime*, using a 3-m long, 32-mm ID facility with a coaxial injector. The shape of the gas-liquid interface would depend on the phase flow rates and in some works it was associated with the roughness in single-phase turbulent pipe flows to determine the interfacial shear stress (Belt et al., 2009). Furthermore, it has been observed that the disturbance waves caused liquid entrainment into the core flow, because of the interaction between the liquid and the gas phases, thus affecting the interfacial shear friction that influences the pressure drop, the two-phase transfer of momentum, mass and heat (Ishii and Grolmes, 1975; Wallis, 1970; Azzopardi, 1997).

Several studies in the literature characterized, analyzed and proposed correlations and models for different inclinations (horizontal, inclined and vertical) of the two-phase annular flow (Alekseenko and Nakoryakov, 1995; Azzopardi, 1986; Fershtman *et al*., 2020; Pan and Hanratty, 2002; Pan *et al.*, 2015; Wang *et al*., 2020; Zabaras *et al*., 1986; Zhao *et al.*, 2013). Ju *et al.* (2015) proposed a new model for upward vertical annular flow that considers pressure, superficial velocities and viscosity of the phases to predict the liquid film thickness. The authors found out that the film thickness is a function of phase Weber numbers. Likewise, Pan *et al.* (2015) experimentally studied and modeled the disturbance wave height of upward annular flow in 25.4-mm ID with measurements at 115D and using a porous mixer as the inlet. Cherdantsev et al. (2021) analyzed the development and interaction of individual disturbance waves in downward vertical annular flow in a 11.7-mm, 650-mm long (~56D) working section, also injecting the liquid as a film to induce annular flow.

Thus, the most common experimental setups available in the literature to evaluate downward vertical annular flow have limited lengths and induce the annular flow from the inlet. In this context, the focus of this article is to analyze the behavior of liquid films in air-water vertical downward annular flow in a 26-mm ID, 14-m long pipe. The influences of downstream evolution in two test sections placed 90D and 335D apart from the outlet of the flow conditioner and the influence of two flow conditioners will be investigated.

2. METHODOLOGY

An apparatus to realize the experimental tests in air-water annular flow was designed. The apparatus has a 26-mm ID, 14-m long test section made of transparent Plexiglas, as the scheme in Figure 1 shows. Special care was taken in obtaining the alignment (90°) of the pipe test sections. The working fluids used in the tests were air and water at room conditions. Twenty-one (21) combinations (C0#) of gas (J_G) and liquid (J_L) superficial velocities ranging from 0 m/s to 20 m/s and 0.05 m/s to 0.25 m/s, respectively, were used in the experiments, as presented in Table 1.

All those 21 combinations fall into the annular flow pattern, as plotted on the flow map proposed by Barnea, Shoham and Taitel (1982), see Figure 2(a). Figure 2 (b) and (c) show a snapshot of two combinations of superficial velocities and both the liquid film and the presence of waves can be observed.

Water from a tank is pumped to the circuit line where a Coriolis flowmeter monitors the liquid flow rate and temperature. Two different types of flow conditioners were used during the tests, both with 0.7 m of length, to evaluate the influences of phase injection on the liquid film features and on the downstream evolution of the flow. The first flow conditioner, named coaxial flow conditioner (FC1), injects the phases coaxially into the main pipe section of tests. The gas, whose flow rate is also measured by a Coriolis flowmeter, is supplied by a tube into the core while the liquid is injected until a ring-shaped reservoir is filled. This reservoir is mounted coaxially to the gas-supply tube, and the liquid flows as a film wetting the wall of the flow conditioner. The second conditioner, named as elbow flow conditioner (FC2), is a tube which also injects gas into the core while the liquid enters through an elbow into the flow conditioner, as depicted in Figure 1. The twenty-one combinations of phase superficial velocities were repeated three (3) times for each flow conditioner so that the repeatability of the experimental results could be verified.

The conductance sensor (CS), placed in two different test-sections (TS1, TS2) at approximately 2.4 m (~90D) and 8.8 m (~335D) from the flow conditioner, measures the liquid thickness evolution in time at two channels (CH1 and CH2) separated by 35 mm. Each channel is composed of two ring electrodes (the receiver and the transmitter) installed concentrically in the cross-section of the pipe. The conductance sensor was previously calibrated by inserting a non-conductive cylinder concentrically into the pipe to simulate the gas core of the annular flow. Thus, the relationship between the known liquid thickness and the sensor output is achieved within the range of the liquid thickness varying between 0.1 mm and 13 mm (pipe entirely filled with water). Technical details about the calibration of the conductance sensor can be found in Dos Santos *et al.* (2021). The CS measurements from the two test sections will be used to evaluate the behavior of the annular flow in the downstream axial direction. A review on the sensing principle of the CS used in this work is given by Shi *et al.* (2020). The data acquisition frequency was 10 kHz with a sampling time of 30 s. A high-speed camera was used to visualize the annular flow and provide qualitative information to corroborate the analysis in this work. The time recorded for each experimental combination of J_L and J_G was 10 s with a frequency of 300 Hz.

Initially, for the measurements using the FC1, the camera was deployed at TS2, positioned 0.4 m after the CS, whereas for the measurements using the FC2 the camera was placed at TS1 positioned 0.4 m before the CS, as depicted in Figure 1.

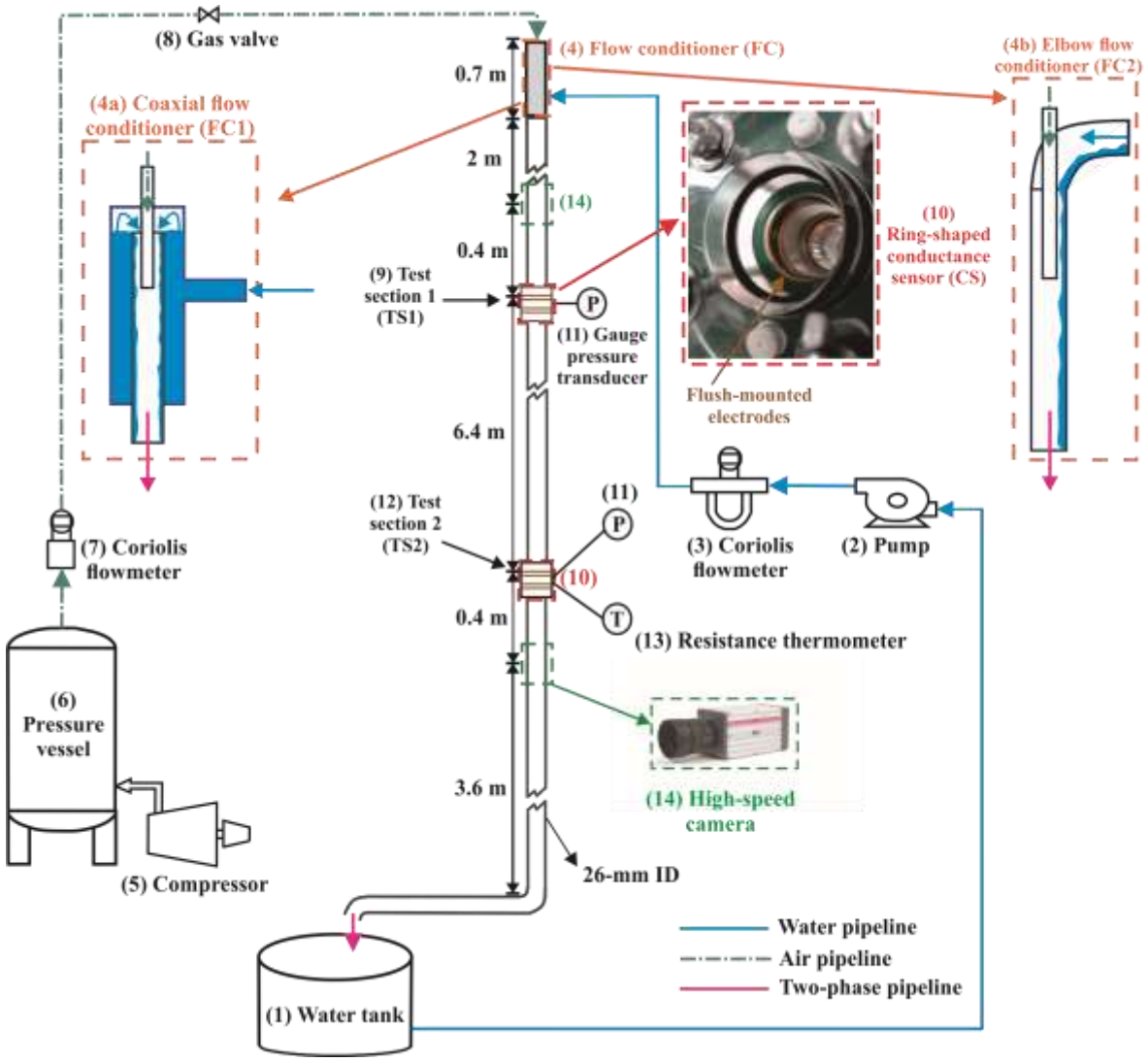

Figure 1- Schematic of the experimental apparatus used in the air-water downward vertical annular flow tests.

Table 1 – Combinations of phase superficial velocities used in the experimental tests.

Combination	J_L [m/s]	J_G [m/s]	Combination	J_L [m/s]	J_G [m/s]	Combination	J_L [m/s]	J_G [m/s]
C01	0.050	10	C08	0.050	15	C15	0.050	20
C02	0.075	10	C09	0.075	15	C16	0.075	20
C03	0.100	10	C10	0.100	15	C17	0.100	20
C04	0.125	10	C11	0.125	15	C18	0.125	20
C05	0.150	10	C12	0.150	15	C19	0.150	20
C06	0.200	10	C13	0.200	15	C20	0.200	20
C07	0.250	10	C14	0.250	15	C21	0.250	20

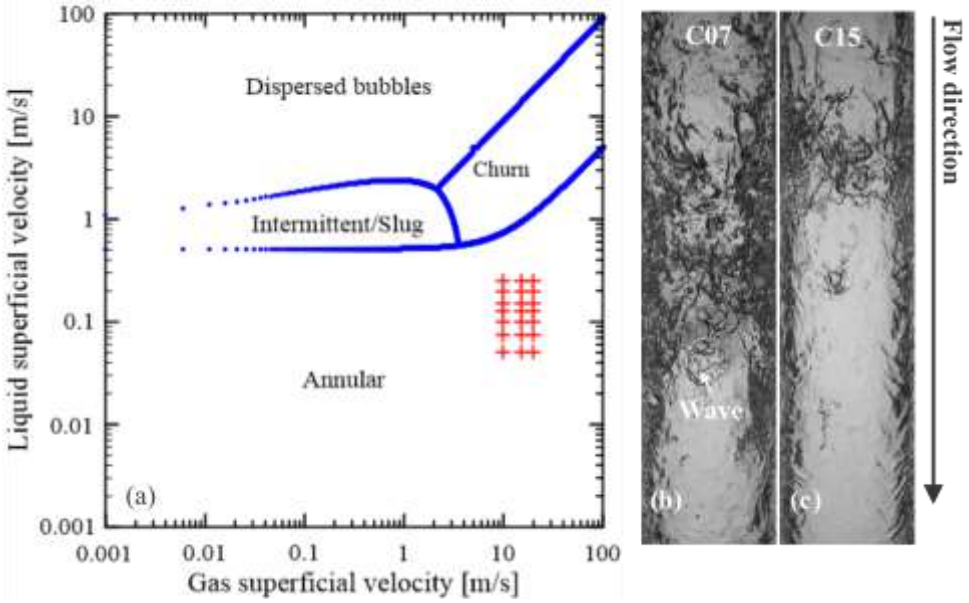

Figure 2- Experimental combinations of phase superficial velocities. (a) Plotted on the flow pattern map proposed by Barnea *et al.*, (1982) for air-water vertical downward flow at 26 mm I.D. (b) and (c) are snapshots of air-water annular flow: (b) C07-J_L=0.25 m/s; J_G=10 m/s and (c) C15-J_L=0.05 m/s; J_G=20 m/s.

3. RESULTS

This section presents the main results obtained in this work aimed at evaluating the downstream evolution and the effects of the flow conditioner in downward vertical air-water annular flows. Initially, the evolution in the axial direction and the influence of the gas and liquid superficial velocities will be evaluated from the measurements using the coaxial flow conditioner (FC1) at TS1 (~90D) and TS2 (~335D). Moreover, the influence of the flow conditioner will be analyzed by comparing the liquid film properties between the two flow conditioners used in this study.

3.1 Downstream flow evolution influence

The annular flow pattern presents an irregular gas/liquid interface with the presence of waves (disturbance waves and ripples) and bubble entrainment into the liquid film, as can be observed in Figure 2 (b) and (c). These waves were formed because of the gas shearing action on the interface. Figure *3* shows the liquid thickness time-signals for the twenty-one combinations of annular flow using the coaxial flow conditioner (FC1) at TS2. The presence of sharp peaks can be observed when the liquid thickness time signals are analyzed. Those peaks represent the disturbance waves and for some combinations of phase superficial velocities can appear ripples in the interface between the peaks. Furthermore, depending on the combination of phase superficial velocities the disturbance waves can be more frequent and with changes in their shape concerning their amplitudes and lengths that fluctuate with time. It is clear from Figure *3* that the frequency of the disturbance waves (DW) increases with the phase superficial velocities. In the figures from the left to the right in row order, the increase of the DW frequency due to the increase of liquid superficial velocity for a fixed gas superficial velocity can be observed, whereas in the column of figures from the upper to the bottom the DW frequency increases because the gas superficial velocity keeps the liquid superficial velocity constant.

Figure 4 shows the characteristics of the liquid film obtained with the coaxial flow conditioner (FC1) at TS1 and TS2 that can provide a quantitative comparison between these features concerning the evolution of the flow in the axial direction. Average liquid thicknesses as a function of the phase superficial velocities are presented in Figure 4 (a). It can be observed that the average liquid thickness is slightly affected by the downward axial position of the flow and tends to be thinner at TS2, with the major variation observed for the highest phase superficial velocities (C21-J_L=0.25 m/s; J_G=20 m/s), with a maximum percentage deviation of -7% between TS1 and TS2. The average liquid thickness has a well-defined trend regarding the phase superficial velocities and increases with the increase in the liquid superficial velocity while J_G remains constant, and the opposite effect (reduction of the average liquid thickness) was also observed with an increase in the gas superficial velocity.

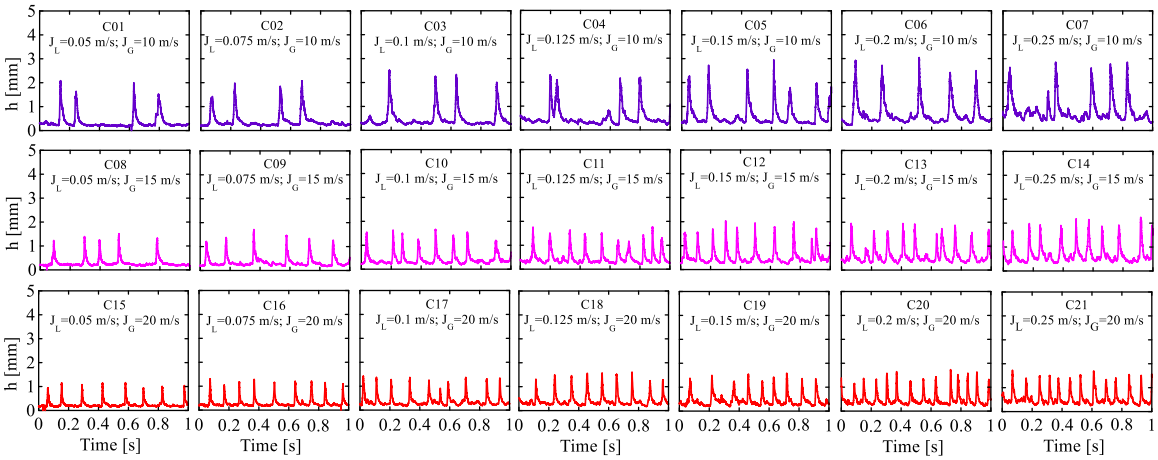

Figure 3 – Liquid thickness time signal for all combinations of air-water superficial velocities of annular flow with the coaxial flow conditioner (FC1) at test section 2 (TS2).

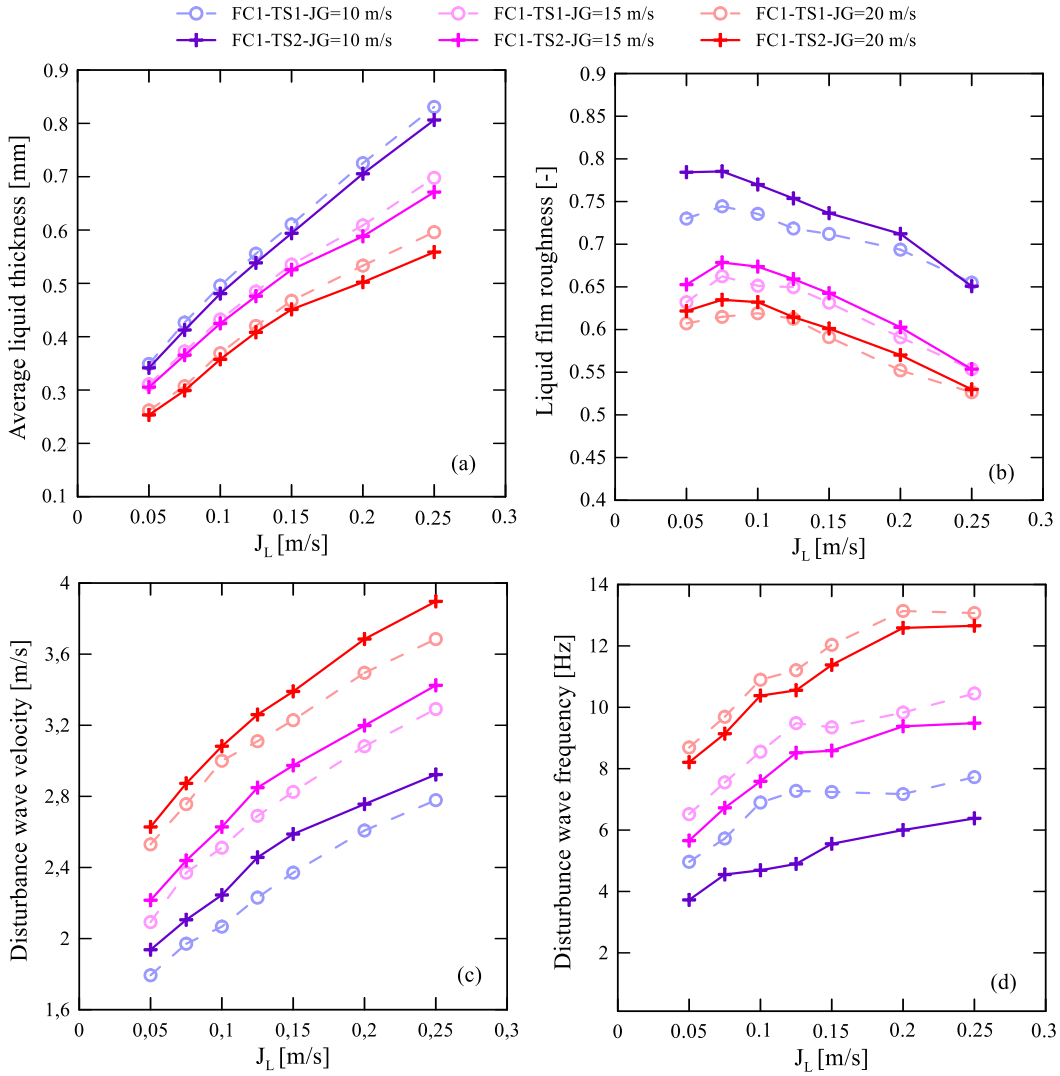

Figure 4 – Measurement of the liquid film features in downward vertical air-water annular flow using the coaxial flow conditioner (FC1) at both test sections (TS1 and TS2) as a function of phase superficial velocities: (a) average liquid thickness, (b) liquid film roughness (ratio between liquid film standard deviation and average liquid thickness), (c) disturbance wave velocity, and (d) disturbance wave frequency.

The liquid film roughness, defined in the literature as the ratio between the standard deviation of the liquid thickness and the average liquid thickness (Karaopantsios, Paras and Karabelas, 1989; Zadrazil et al., 2014), has an opposite trend vis-à-vis the liquid superficial velocity in comparison with the behavior presented in Figure 4 (a). The liquid film roughness decreases with the increase in J_L, as presented in Figure 4 (b), keeping the same effect regarding the J_G observed in the average liquid thickness, as described before. Besides, an opposite behavior is also observed concerning the difference between film roughness at TS1 and TS2, as the liquid film roughness tends to increase in the axial direction (TS2). A maximum percentage deviation of +7% was observed for the lowest combination of phase superficial velocities (C01).

The disturbance wave (DW) velocity is presented in Figure 4 (c). This velocity is obtained by a cross-correlation function between the time signal measurements of each channel of the conductance sensor. Note that the DW velocity is higher at TS2 and increases with both J_L and J_G. A maximum percentage deviation of +10% was observed for the DW velocity between the TS1 and TS2. Apart from the DW velocity, the DW frequency is also affected by the phase superficial velocities, with the same influence observed for the DW velocity, with the opposite effect regarding the evolution of the flow, being the DW frequency smaller at TS2 than at TS1, as depicted in Figure 4 (d). The DW frequency presents a more significant variation between the TS1 and TS2 for the smallest combinations of gas superficial velocities (C01-C07), with a maximum percentage deviation of -50% for the C04 at TS2. The disturbance wave frequency was determined by directly counting, calculated by the number of waves to sampling time ratio. The threshold used for the DW identification was the substrate film that was determined by all local minima of the liquid thickness time signal.

3.2 Effect of the flow conditioner

The effects of how the phases are fed into the pipe on the annular flow evolution in the axial direction are presented in Figure 5. Two combinations are used to provide an overview of the range of J_L and J_G used in the experiments described in this work: the air-water annular flow with J_L=0.075 m/s and J_G=10 m/s (C02) and the C21 with J_L=0.25 m/s and J_G=20 m/s, with the latter combination presenting the highest values of phase superficial velocities used herein.

First, analyzing the interfacial morphology of the liquid thickness for the tests using the coaxial flow conditioner (FC1), which induces the annular flow formation, it can be observed by qualitative comparison between the liquid thickness time signals that the DW activity tends to change in the downstream direction of the flow for the C02, as shown in Figure 5 (a) and (b), where disturbance waves are the peaks in the liquid thickness time signals. The main variation observed in the C02 is in the DW frequency (a decrease in the wave frequency at TS2), as presented before in Figure 4 (d). A reduction in the DW frequency is also detected in C21, but this effect is not noticed by a qualitative comparison between the liquid thickness time series.

Similarly, Figure 5 (e)-(h) illustrate the liquid thickness time signals for the elbow flow conditioner (FC2). In the experiments using the FC2 at TS1, the liquid thickness time signal for C02 is quite different, as shown in Figure 5 (e), in comparison with this same combination using the FC1 at TS2, Figure 5 (a). Observing the snapshots taken during the experimental tests it was possible to confirm that at the TS1 the flow is not annular (the liquid flows only on one side of the pipe wall), as shown in

Figure *6* (a). Hence, for this combination of phase superficial velocities the elbow flow conditioner affects the flow at TS1, an influence that is also detected for other combinations of phase superficial velocities. However, with the evolution observed downstream, at TS2 the flow reaches the annular flow pattern as it can be confirmed by the liquid thickness time signal and visual observation, as shown in Figure 5 (a) and (b). On the other hand, C35 is not affected by the FC2 and this is probably due to the interfacial shear stress effects of the highest gas superficial velocity (J_G=20 m/s) that causes the formation of the annular flow regardless of the influence of the flow conditioner, showing that the influence of the gas superficial phase is more significant than the effects of the flow conditioner. Moreover, the combination of phase C35 was also confirmed as annular flow by snapshots of the flow at TS1. The occurrence of bubble entrainment into the liquid film (both in the film substrate and in the disturbance waves) and entrainment of droplets to the gas core were visually observed for all combinations of J_L and J_G and both flow conditioners at TS2. The bubbles in the DW, located in the darker regions in

Figure *6* (c) and (d), are affected by the gas flow rate.

Figure 7 shows the result of average liquid thickness, roughness film, disturbance wave velocity and disturbance wave frequency for both flow conditioners experimentally analyzed in this work at TS2 (~335D). Comparing the results, a good agreement between the features of the annular flow can be observed, and it can be verified that for all combinations of phase superficial velocities investigated the downward vertical annular flow characteristics are not affected by the type of flow conditioner at 335D from the inlet. The maximum deviation observed in Figure 7 was 4% for the average liquid thickness, liquid film roughness, and DW velocity, and 6.5% for DW frequency. These results serve to demonstrate that the downward annular flow is independent of the type flow conditioner in a test section placed at 335D from the inlet, for annular flow conditions and flow conditioners analyzed in the present work.

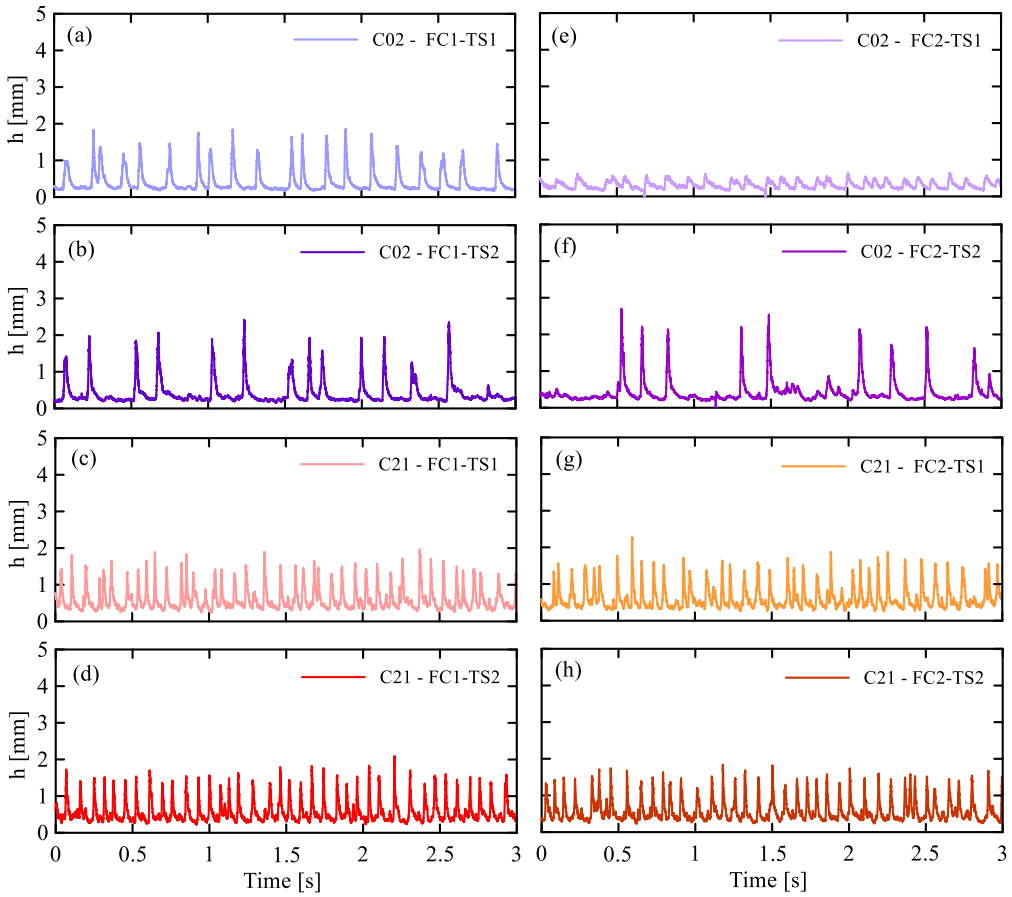

Figure 5- Liquid thickness time signal measurements (h) for two combinations of phase superficial velocities, C02-J_L=0.075 m/s; J_G= 10 m/s and C21-J_L=0.25 m/s; J_G=20 m/s: (a)-(d) experimental results using the coaxial flow conditioner (FC1) and (e)-(h) experimental results using the elbow flow conditioner (FC2) in the test section placed at 90D (TS1) and 335D (TS2) from the flow conditioner outlet.

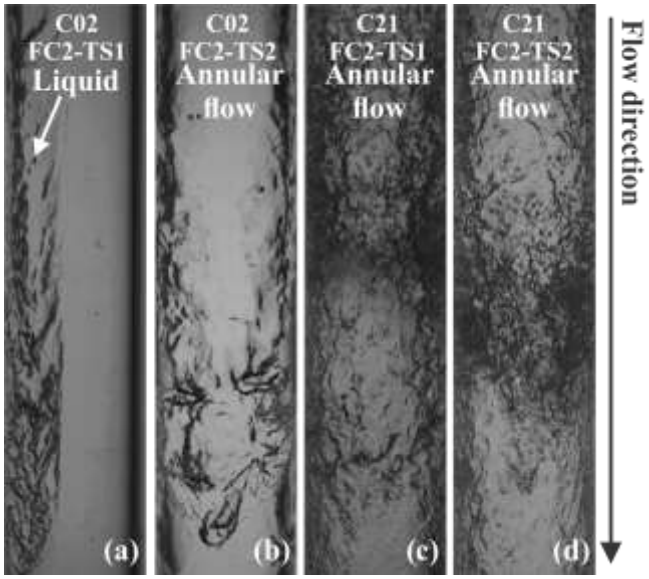

Figure 6 – Snapshots of the experimental combinations at the different test sections used to investigate the evolution of the downward annular flow using the elbow flow conditioner (FC2): (a)-(b) C02-J_L=0.075 m/s; J_G= 10 m/s at test section 1 (TS1) and test section 2 (TS2), respectively, and (c)-(d) C21-J_L=0.25 m/s; J_G=20 m/s at TS1 and TS2, respectively.

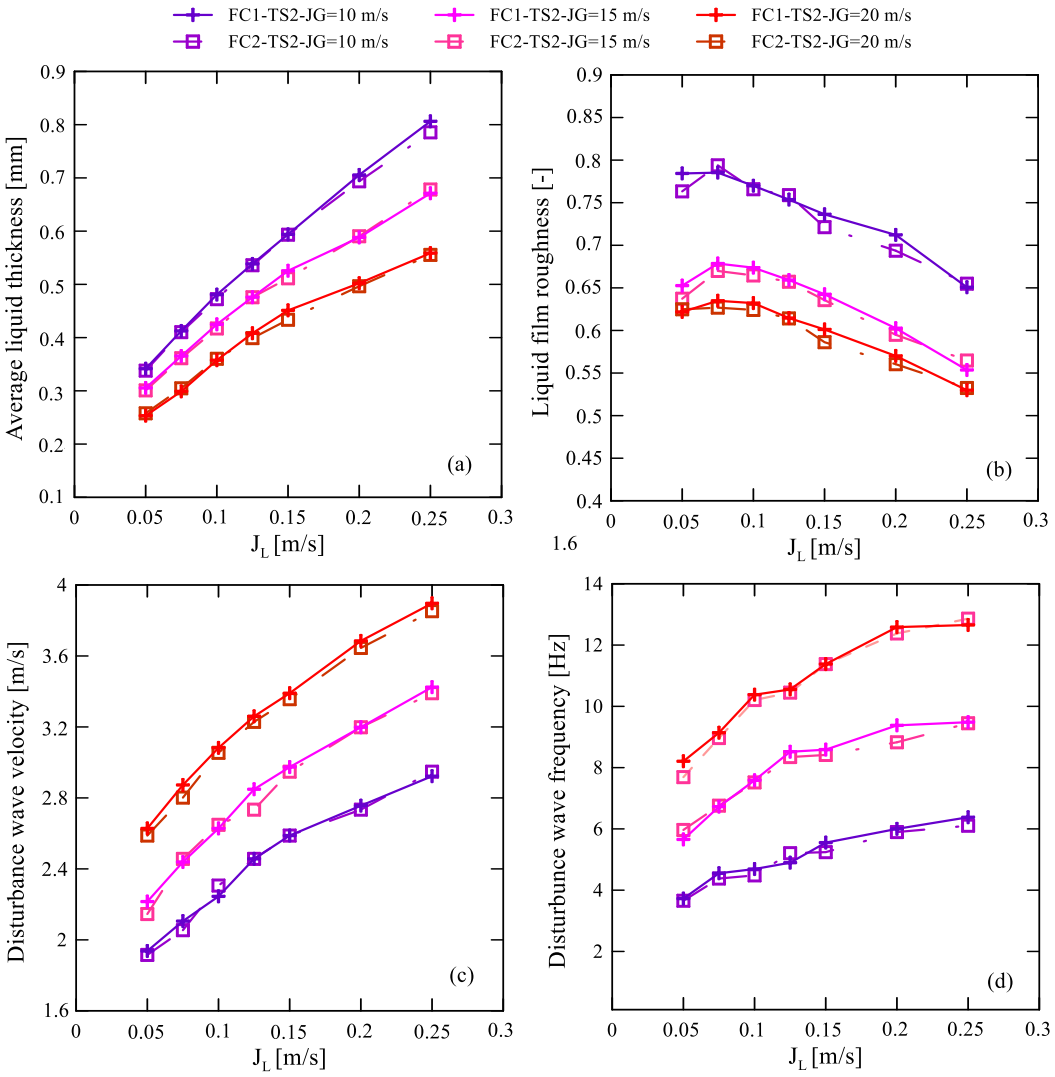

Figure 7 - Measurement of the liquid film features in downward vertical air-water annular flow using the coaxial flow conditioner (FC1) and the elbow flow conditioner (FC2) at test sections 1 and 2 (TS1 and TS2) as a function of phase superficial velocities: (a) average liquid thickness. (b) liquid film roughness (ratio between liquid film standard deviation and average liquid thickness), (c) disturbance wave velocity, and (d) disturbance wave frequency.

4. CONCLUSIONS

In this work, an experimental analysis of liquid film thickness in downward vertical air-water annular flows was carried out using a non-intrusive conductance sensor and a high-speed camera in a 26-mm ID, 14-m long pipe. From the experimental results, the influences of downstream evolution in the axial direction of the flow and the effects of how the phase is injected into the pipe were evaluated. In summary, the major findings of this work are:

- For all features of annular flow herein evaluated, namely the average liquid thickness, the roughness liquid film, the disturbance wave velocity, and the disturbance wave frequency, changes in the downstream direction were observed between the two tests sections analyzed.
- The effects of the flow conditioner that not induce the formation of annular flow were observed only at the test section placed near the outlet of the flow conditioner, where for some combinations of phase superficial velocities the annular flow is not formed. However, these results demonstrated that for a test section placed at 335D from the flow conditioner the downward annular flow was not affected by the entrance of the phases.

5. ACKNOWLEDGEMENTS

The authors would like to express their gratitude for the financial support given by PETROBRAS/CENPES.

6. REFERENCES

Alekseenko, S. V., Nakoryakov, V.E., 1995. Instability of a liquid film moving under the effect of gravity and gas flow. Int. J. Heat Mass Transf. 38, 2127-2134. https://doi.org/10.1016/0017-9310(94)00326-Q

Azzopardi, B.J., 1997. Drops in annular two-phase flow. Int. J. Multiph. Flow 23, 1-53.

Azzopardi, B.J., 1986. Disturbance wave frequencies, velocities and spacing in vertical annular two-phase flow. Nucl. Eng. Des. 92, 121-133.

Barnea, Dvora; Shoham, Ovadia and Taitel, Y., 1982. Flow Pattern Transition for Vertical Downward Two-Phase Flow.

Belt, R.J., Van't Westende, J.M.C., Portela, L.M., 2009. Prediction of the interfacial shear-stress in vertical annular flow. Int. J. Multiph. Flow 35, 689-697. https://doi.org/10.1016/j.ijmultiphaseflow.2008.12.003

Cherdantsev, M. V., Isaenkov, S. V., Cherdantsev, A. V., Markovich, D.M., 2021. Development and interaction of disturbance waves in downward annular gas-liquid flow. Int. J. Multiph. Flow 138, 103614. https://doi.org/10.1016/j.ijmultiphaseflow.2021.103614

Chu, K. J. and Dukler, A.E., 1975. Statistical Characteristics of Thin, Wavy Films III. Structure of the Large Waves and their REsistance to Gas Flow. AIChE J. 21, 583-593.

Fershtman, A., Barnea, D., Shemer, L., 2021. Wave identification in upward annular flow - a focus on ripple characterization. Int. J. Multiph. Flow 137, 103560. https://doi.org/10.1016/j.ijmultiphaseflow.2021.103560

Fershtman, A., Robers, L., Prasser, H.M., Barnea, D., Shemer, L., 2020. Interfacial structure of upward gas–liquid annular flow in inclined pipes. Int. J. Multiph. Flow 132, 103437. https://doi.org/10.1016/j.ijmultiphaseflow.2020.103437

Hewitt, G F and Hall-Taylor, N.S., 1970. Annular Two-Phase Flow. Pergamon Press, Oxford.

Ishii, M., Grolmes, M.A., 1975. Inception Criteria for Droplet Entrainment in Two Phase Concurrent Film Flow 21.

Ju, P., Brooks, C.S., Ishii, M., Liu, Y., Hibiki, T., 2015. Film thickness of vertical upward co-current adiabatic flow in pipes. Int. J. Heat Mass Transf. 89, 985-995. https://doi.org/10.1016/j.ijheatmasstransfer.2015.06.002

Karaopantsios T.D., P.S.., Karabelas A.J, 1989. Statistical characteristics of free falling films at high Reynolds numbers. Int. J. Multiph. Flow 15, 1-21.

Lokanathan, M., Hibiki, T., 2016. Flow regime, void fraction and interfacial area transport and characteristics of co-current downward two-phase flow. Nucl. Eng. Des. 307, 39-63. https://doi.org/10.1016/j.nucengdes.2016.05.042

Pan, L., Hanratty, T.J., 2002. Correlation of entrainment for annular flow in horizontal pipes. Int. J. Multiph. Flow 28, 385-408. https://doi.org/10.1016/S0301-9322(01)00074-X

Pan, L.M., He, H., Ju, P., Hibiki, T., Ishii, M., 2015. The influences of gas-liquid interfacial properties on interfacial shear stress for vertical annular flow. Int. J. Heat Mass Transf. 89, 1172-1183. https://doi.org/10.1016/j.ijheatmasstransfer.2015.06.022

Qiao, S., Mena, D., Kim, S., 2017. Inlet effects on vertical-downward air–water two-phase flow. Nucl. Eng. Des. 312, 375-388. https://doi.org/10.1016/j.nucengdes.2016.04.033

Santos, E.N., Santana, A.L.B., Reginaldo, N.S., Wrasse, N., Silva, M.J., Morales, R.E.M., 2021. Evaluation of Conductance Flow Sensor for Liquid Thickness Measurement in Annular Flow i, 1-4.

Shi, X., Tan, C., Dong, F., dos Santos, E.N., da Silva, M.J., 2020. Conductance Sensors for Multiphase Flow Measurement: A Review. IEEE Sens. J. 1-13. https://doi.org/10.1109/JSEN.2020.3042206

Wallis, G.B., 1970. Annular Two-Phase Flow Part 1 : A Simple Theory 59-72.

Wang, J., Xu, Y., Zhang, T., 2020. Measurement and prediction on the liquid film thickness of swirling annular flow. Meas. Sensors 10-12, 100020. https://doi.org/10.1016/j.measen.2020.100020

Webb, D. R. and Hewitt, G.F., 1975. Downwards Co-current Annular Flow. Int. J. Multiph. Flow 2, 35-49.

Zabaras, G., Dukler, A.E., Moalem-Maron, D., 1986. Vertical upward cocurrent gas-liquid annular flow. AIChE J. 32, 829-843. https://doi.org/10.1002/aic.690320513

Zadrazil, I., Matar, O.K., Markides, C.N., 2014. An experimental characterization of downwards gas-liquid annular flow by laser-induced fluorescence: Flow regimes and film statistics. Int. J. Multiph. Flow 60, 87-102. https://doi.org/10.1016/j.ijmultiphaseflow.2013.11.008

Zhao, Y., Markides, C.N., Matar, O.K., Hewitt, G.F., 2013. Disturbance wave development in two-phase gas-liquid upwards vertical annular flow. Int. J. Multiph. Flow 55, 111-129. https://doi.org/10.1016/j.ijmultiphaseflow.2013.04.001

7. RESPONSIBILITY NOTICE

The author(s) is (are) the only responsible for the printed material included in this paper.